

**On the possibility of replacement of calcium carbonate by  
a high-performance, economically viable filler in  
polyethylene composites**

Mohammadnabi Hesabi <sup>1</sup>, Shane Brennan <sup>1</sup>, Quentin Boulard <sup>2</sup>, Francois Le  
Blanc <sup>3</sup> and Ian Major <sup>1,\*</sup>

<sup>1</sup>Material Research Institute, Athlone Institute of Technology, Dublin Road, Athlone, Ireland,  
N37 HD68

<sup>2</sup>Polytech'Montpellier, Material Department, Montpellier II University, CC 419, Place E.  
Bataillon, 34095 Montpellier, France

<sup>3</sup>CESI, Engineering School, Boulevard de l'Université, 44600 Saint-Nazaire, France

\* Corresponding author: Tel: +353-906-48-3084

Email: [imajor@ait.ie](mailto:imajor@ait.ie)

## **Abstract**

Calcium carbonate ( $\text{CaCO}_3$ ) is frequently added to polyethylene (PE) as a filler to reduce costs. An alternative to  $\text{CaCO}_3$ , calcium fluoride ( $\text{CaF}_2$ ) was proposed in this research. PE/ $\text{CaCO}_3$  and PE/ $\text{CaF}_2$  composites in a wide composition range (0-60 wt.%) were prepared through a parallel twin screw extruder. Results indicated better interaction of  $\text{CaF}_2$  with PE matrix which improved samples yield stress. Statistical analysis showed the filler type was more influential factor on the yield stress while filler loading was not a statistically significant one. In contrast, crystallinity was strongly depended on the filler loading. The dynamic mechanical and rheological investigations revealed that PE/ $\text{CaF}_2$  composites had higher stiffness at ambient temperature and possessed lower viscosity below 40 wt% of filler loading compared to PE/ $\text{CaCO}_3$  which could reduce the processing cost. Therefore, regarding its low price and good functional properties,  $\text{CaF}_2$  can be a promising alternative to  $\text{CaCO}_3$ .

**Keywords:** Calcium fluoride, circular economy, statistical analysis, fillers, injection molding

## 1. Introduction

According to Geyer et al. over 100 million tons of polyethylene (PE) based resins are produced annually to satisfy global demand making it the most used polymer (1), accounting for 34 % of the total thermoplastic resin use worldwide. This most versatile of polymers, lends itself to many consumer sectors, ranging from refuse bags to foamed products and medical devices (2–6).

Ease of processability has allowed PE to dominate many commercial items, particularly thin films used in refuse bags and agriculture film (7–9). However, our focus for PE is in injection molding, and the anticipated growth of the resin in this sector (8). Cost-effective thermal processing is vital in achieving competitiveness in a crowded market place, and it is a material's melt behavior which dominating the processing cost factors (10,11). Energy input in conjunction with polymer resin price are among core instigators regarding PE and low-cost filler research (10,12,13). If the addition of filler can achieve a reduction in either of these parameters while still upholding mechanical performance or even improving upon a material's mechanical attributes, then it can give significant economic benefits for manufacturers.

Calcium carbonate ( $\text{CaCO}_3$ ) is one of the most common substances found on earth (14). It is frequently added to PE products as a filler (15) to reduce costs, either via decreasing the processing energy and/or the cost of bulk materials (16–19). An alternative to  $\text{CaCO}_3$ , calcium fluoride ( $\text{CaF}_2$ ) is proposed in this research paper.  $\text{CaF}_2$  is a commonly occurring substance on the Earth's surface and is often mined as the gangue material fluorite particularly from zinc and lead mines (17). Synthetic  $\text{CaF}_2$ , the focus of this study, is a byproduct of the semiconductor industry from the removal of fluoride from wastewater (18). While  $\text{CaF}_2$  can be utilized as a component in some niche product areas, in particular as steel flux (19) and the glass and lens markets (21–24), large quantities of recovered synthetic  $\text{CaF}_2$  exist as a consequence and efforts must be made to divert this byproduct away from landfill in our

growing Circular Economy. Under best scrutiny of this study, no evidence of using  $\text{CaF}_2$  as a significant replacement for  $\text{CaCO}_3$  as a PE filler in the manufacturing of injection molded parts exists. This study will investigate the feasibility of using raw  $\text{CaF}_2$  as a possible alternative to  $\text{CaCO}_3$  master batch as a filler in PE.

The mechanical properties of a polymer is frequently reported as being negatively affected by the addition of an inorganic filler (25–27). In this regard, the filler loading was investigated in a wide range, namely 0-60 wt.%, in this study. Strain-controlled deformation is the most prolific tool in determining the modulus of test specimens, and the importance of strain rate cannot be underestimated (28–31). The composite systems were therefore deformed under two strain rates varied by a factor of twenty. Yield stress was a primary comparison factor along with Young's modulus. Thermal behavior can be a significant indicator of how a material system will perform under loading (32,33). Differential scanning calorimetry techniques were employed to yield crystallinity changes of PE composites before and after hot melt extrusion processing.

The addition of solid particles exhibiting largely non-viscoelastic behavior can pose challenging obstacles concerning melt processing and decrease processability. Rheometric data across a temperature ramp and at isothermal processing temperatures can give a reasonable prediction of processing performance in traditional extrusion and molding equipment (32,34). In order for this filler comparison study to have a valuable and valid objectives a statistical approach to outcomes was sought. After characterizations were completed, both  $\text{CaCO}_3$  and  $\text{CaF}_2$  were pitted against each other under the scrutiny of ANOVA. Filler type was not compared in isolation however, filler quantity underwent statistical investigation as the correlation between the wt% loading and composite saturation is also of primary concern.

## **2. Experimental**

## *2. 1 Materials and Sample Preparation*

The PE resin used in this study was Lotrene Q TR131, which is a medium density hexane copolymer PE resin with the melt index of 0.2 g/10min (@190 °C/2.16 kgs). The material was received in sealed double layer bags and was used without any further processing. CaCO<sub>3</sub> was received in master batch pellet form Ancal. Co, grade 80. Filler content was observed at 82. 5 wt% calcium carbonate and 17.5 wt% of polyethylene. The CaCO<sub>3</sub> was presented in double layer moisture locked bags and used without further treatment. Recycled CaF<sub>2</sub> was obtained from local mineral sources in its common raw gangue form. The mineral came in a large array of aggregate sizes which was preliminarily sieved to 2mm to allow further lab processing. The material was dried initially in a hot air circulating oven at 80 °C for 24 hours. Then further sorted to 600µm and using a ball mill, it was milled until a uniform consistency was achieved. Material that passed a 300µm sieve was used. The powder was then further dried at 110 °C until a moisture of ≤0.1% was reached. Synthetic CaF<sub>2</sub> has a density of 3.18 g/cm<sup>3</sup>, a Young's Modulus of 75.8 GPa and Bulk Modulus of 82.7 GPa (35). A Leistritz Micro 27, co-rotating, twin screw extruder with a 38:1 length to diameter ratio was used to compound both the CaCO<sub>3</sub> and the CaF<sub>2</sub> with the PE pellet. The extruder had 8 heated barrel zones rising in 10 °C increments from 80 °C at the throat to 160 °C. There were two further heated die zones increasing in 20 °C increments. This left the terminal temperature zone of the extruder at 200 °C. The compounding ratios were achieved by using two volumetric feeders that simultaneously fed the extruder's screws which was set at the rotational speed of 80 RPM. One gravimetric feeder fed PE pellet and the other fed filler material into the extruder through the hopper, both were tested before trials to ensure correct mass per second rate. The filament strand drawn through an ambient temperature water bath and then pelletized using a sharp edge shear-grinder. The wt% of filler to PE used for investigation and the corresponding notations of samples has been shown in Table 1.

An Arburg<sup>TM</sup> ALL-Rounder 370E was used to mould the compounded material. The injection molder had a maximum clamping force of 600 kN, screw diameter of 30 mm and a stroke volume approaching 85 cm<sup>3</sup>. A family type, tool steel, oil cooled mould was used, containing standardized tensile, impact, dynamic mechanical and rheological test specimens in accordance with ISO 294-1 and ISO 6239 geometries. All material were stored in a hot air circulating oven at 60 °C for 24 hours prior to use to remove any residual surface moisture post pelletizing. The temperature profile for molding was 50 °C at the hopper, increasing to 225 °C at the nozzle. Injection speed was optimized at 80 mm/s. The dosage stroke was 55 mm with circumferential screw speed at 350 mm/s. A holding pressure of 1000 bar for 10.4 s was used. Cooling time was set to 35 seconds with a back pressure of 40 bar.

## *2. 2 Characterization*

Thermal characterization of samples were examined by Differential Scanning Calorimetry (DSC) test using a Thermal Analysis [TA] DSC 2920 with a refrigerated cooling system, each batch was tested three times for reproducibility. The samples were weighed out between a 10-12 mg window, and using TA pans were tested without lids. The tests were conducted in a nitrogen gas environment. Initially each sample was heated from 20 °C to 130 °C at 10 °C/min to reduce moisture interference at boiling point and to remove PE's thermal history. The samples were then cooled to -50 °C at 10 °C/min and held isothermally for 1 min. The characterization curve used a 10 °C/min ramp between -50 °C and +170 °C.

Tensile testing was conducted on a Zwick Roell Z010. Two strain rates of 5 mm/min and 100mm/min were used. Tests were stopped at 20% strain value or until mechanical failure occurred which was determined as an 80% drop off from max stress point. Five samples per batch for each strain rate were tested for tensile strength and Young's modulus.

The gold sputtered cryogenically fractured-surfaces of samples were explored via scanning electron microscope (SEM, TESCAN-MIRA//FE-SEM).

Dynamic mechanical analysis (DMA) tests were conducted on a Thermal Analysis Q800 DMA at a heating rate of 3 °C/min. A single cantilever clamp orientation was used. Each sample was subjected to a temperature ramp between -110 to 100 °C at a sinusoidal displacement of 12 µm at 1 Hz.

The rheological properties of samples were studied using the Discovery Hybrid Rheometer 2, with oven heating assembly (DHR-2, TA Instruments). The samples were placed between two flat plates of 25 mm diameter after calibration of the zero gap. For the analysis of pure polymer and composite, a frequency sweep was conducted at 2 % strain at 230 °C with a gap width of 1 mm. The sweep underwent frequency starting at 0.01 to 100 Hz. Applied strain at 2 was within the linear viscoelastic region of all the samples.

### **3. Results and Discussion**

#### *3.1 Thermal analysis*

Figure 1 compares the non-isothermal DSC thermograms of virgin PE with some of its calcium carbonate and calcium fluoride-filled composites. The comprehensive results are listed in Table 2. As seen in Table 2, incorporation of CaCO<sub>3</sub> slightly increased the onset and peak temperatures of PE melting however, CaF<sub>2</sub> had an adverse effect. Nevertheless, incorporation of the fillers into PE was not significantly affected the melting characteristics. For all sample, a sharp single melting peak with a vague shoulder at lower temperatures was observed. In general, for semi-crystalline polymers such as polyethylene, the thickness, and perfection of crystals determine the level of melting temperature (36). Therefore, the existence of the shoulder at the lower temperatures can be attributed to the non-uniformity and imperfection state of crystals in the polyethylene. Due to higher thermal conductivity of calcium fluoride than calcium carbonate, it was expected that the CF composites were exposed to the lower amount of enthalpy which could alter the degree of crystallinity. Figure 2 illustrates the effect of filler type and content on the enthalpy and crystallinity of the samples. As shown in Figure

2-a, by increasing the filler content the enthalpy of composites dwindled for both systems. The decline was more distinctive at the 20 wt% of filler content for both composites. Since organic fillers increase the thermal conductivity of polymers melt, the decline in the enthalpy of composites by increasing the filler content was a predictable trend. However, in spite of the higher thermal conductivity of calcium fluoride, the enthalpy of PF composites was generally higher than the PC ones in the same filler content. To find more about this, a statistical analysis was applied to DSC results. Actually, by applying the statistical method, the conclusions will be objective as opposed to judgmental in nature (37).

In this regard, an experimental design based on general full factorial method was employed. Two treatment factors, namely filler content and filler type at 6 and 2 levels, respectively, were considered with three replications. The results were examined using analysis of variance technique (ANOVA). There are two main assumptions for the probability distribution of the responses in ANOVA, i.e. independence and normality. Normality assumption can easily be checked using a normal probability plot. If the hypothesized distribution adequately describes the data, the plotted points will fall approximately along a straight line. Independence assumption also can be evaluated through plotting response data in time order of data collection. In this regard, any tendency to positive or negative residuals can violate the independence assumption (38). Figure 3 shows the normal probability plot and the plot of residuals vs. observation order for the response of enthalpy. The distribution of points along the straight line and the random distribution of residuals within the observation order indicated that both assumptions were fully satisfied. The results of ANOVA for the confidence interval of 95% have been summarized in Table 3. Since among the observed value of F, just the F-value of filler content is greater than the critical F values ( $F_{0.025,1,24}=5.27$  and  $F_{0.025,5,24}=3.15$ ) the null hypothesis is rejected. It means among the independent variables and their interactions, the only one that had statistically significant effect on the enthalpy changes was the filler



content and the variability of the results of other factors simply was rooted in the natural source of variation such as sampling etc. The same trend was observed in the case of crystallinity (Figure 2-b). By increasing the filler content in both systems the degree of crystallinity fell off, however, the PF composites showed a higher amount of crystallinity in the same amount of filler content. Nonetheless, the ANOVA results revealed that the filler content was the only statistically significant factor (Table 4). In other words, despite their physiochemical differences, both inorganic fillers at the same content have a similar impact on the polyethylene thermal characteristics.

### *3. 2 Mechanical properties*

The yield stress and the Young's modulus of the samples were measured at slow (5 mm/min) and fast (100 mm/min) cross-head speeds, to study the influence of the deformation rate on the mechanical behavior. Table 5 summarizes the results of the tensile tests. Each data is an average of 5 replications. Generally, the increase of the strain speed resulted in higher tensile properties. Similar results have been reported by other researchers as well (39,40). According to the time-temperature superposition principle, the time and temperature correspond with each other. Increasing the strain rate would offer an equivalent effect as the decreasing of temperature has. In other words, high strain rates support the elastic properties of materials while low strain speeds favor the energy-damping aspects.

Figure 4 illustrates the yield stress and Young's modulus variations of PC and PF composites over the range of filler content. As seen the yield stress and the Young's modulus tended to ascend by increasing the fillers loading. However, PF composites demonstrated greater tensile properties compared with PC ones in the same filler content. Again, to provide an objective conclusion over the tensile results, the ANOVA method was employed. Table 5 and 6 summarize the result of ANOVA for yield stress and Young's modulus responses, respectively. Interestingly, according to table 5, the influence of filler content on the yield stress of

composites was not statistically significant while the most influential factor was the strain speed. Moreover, from the statistical point of view, except for the interaction of filler content and strain speed, the effect of other interactions between the independent factors on the yield stress was negligible. However, it is obvious from Table 6 that all independent factors even their interactions- except for interaction of filler type and strain speed- had a significant effect on Young's modulus. The better mechanical performance of PF samples compared to PC ones can be attributed to the better interfacial interaction between PE matrix and  $\text{CaF}_2$  which was clear through SEM images (Figure 5) As seen in Figure 5-a and b, a distinct gap between  $\text{CaCO}_3$  particles and PE matrix was obvious. Whereas the  $\text{CaF}_2$  particles were well-covered by the matrix and no gap or discontinuity in interfacial area was observed. While the nature of the interfacial interaction between  $\text{CaCO}_3$  and polymers has been thoroughly investigated (41), the information on the interaction of  $\text{CaF}_2$  particles and polymers are limited. Leija et al. compared the effect of pristine  $\text{CaF}_2$  and surface modified one on the crystallization behaviour of PET (42). For both fillers, the filler particles were well embedded in PET matrix and surface modification only decreased the filler tendency for agglomeration. Leeuw et al. showed that  $\text{CaF}_2$  is a strong ionic catalyst with a potential of formation H-F hydrogen bonding (43). It seems that the good wettability properties of  $\text{CaF}_2$  in polymer matrix can be attributed to its possibility in forming hydrogen bonds between F atom in the filler and hydrogen groups in polymers.

This result shows that calcium fluoride can be considered as a potential filler for polyolefins where both mechanical performance and the production cost are concerned.

### *3. 3 Dynamic mechanical analysis*

Figure 6-a presents the storage modulus of PF composites as a function of temperature. For composites with the filler content lower than 20 wt% the storage modulus did not change significantly compared with virgin PE. While in high-loaded PF composites (more than 20

wt.%) the storage modulus increased over the entire range of temperature as filler content increased. A similar manner was observed for PC composites (results are not shown). Figure 6-b compares the storage modulus of the samples of PC-60, PF-60, and virgin PE. As seen, the storage moduli of composites were higher than the virgin PE over the whole range of temperature, while the storage modulus of PC-60 was higher than PF-60 at minus temperatures and got lower by increasing the temperature above zero. As the performance of the polymer composites at ambient conditions is of interest to industrial applications, Table 7 summarizes the dynamic mechanical characteristics of samples at the ambient temperature. Compared to virgin PE, the stiffness and moduli of the composites at the ambient temperature increased by increasing the filler content. In the meanwhile, PF composites at the ambient temperature presented higher dynamic mechanical properties compared to PC composites. It can be assigned to better interfacial interaction between  $\text{CaF}_2$  particulates and PE matrix as was clear in SEM images. As presented in Table 7, overall PF samples showed lower loss modulus than PC samples at ambient temperature. It seems that better interfacial interaction in PF samples led to more elastic and stronger bonding between the composite constituents resulting in lower loss properties and higher stiffness at ambient temperature.

### *3. 4 Rheological analysis*

Figure 7 and 8 demonstrates storage modulus ( $G'$ ) and the absolute value of complex viscosity ( $|\eta^*|$ ) of PE/ $\text{CaCO}_3$  and PE/ $\text{CaF}_2$ , respectively. It is obvious that the incorporation of each filler resulted in different rheological behavior. Generally,  $\text{CaCO}_3$  increased the dynamic modulus and complex viscosity of PE. However, for samples containing less than 10 wt% of calcium carbonate, the dynamic rheological properties of PE did not seem that affected by filler significantly. While by increasing the  $\text{CaCO}_3$  loading above 20 wt% a distinct increase was distinguishable. Whereas,  $\text{CaF}_2$  in low concentrations lowered the storage modulus and viscosity. Nonetheless, storage modulus and viscosity became greater than PE for the PF

samples containing more than 40 wt.% filler. The relatively similar  $G'$  slopes for PC composites indicates that calcium carbonate particles did not have a strong interaction with each other even at high concentrations. Whereas calcium fluoride incorporation into PE matrix affected the slope of  $G'$  that in fact can be considered as a rheological signature of good interaction of filler and matrix.

By comparing the relative viscosities (normalized viscosity of the composites by the matrix (PE) contribution) of both composites their different rheological behavior will be more obvious. Figure 9 compares the relative viscosities of PC-20, PC-60, PF-20, and PF-60. As can be seen, the lowest and highest viscosities belong to PF-20 and PF-60, respectively. The viscosity of PF-60 tended to rise at low frequencies while in the case of PC-20 and PC-60 the relative viscosity had almost a constant trend over the whole frequency range. The divergence of the relative viscosity of PF-60 at lower frequencies indicates network behavior which is resulted from good interaction of  $\text{CaF}_2$  particles and PE matrix at high concentrations (44). Furthermore, incorporation of  $\text{CaCO}_3$  and  $\text{CaF}_2$  showed opposite effects on the crossover point in dynamic rheology test. Higher amount of  $\text{CaCO}_3$  shifted the crossover points of the samples towards higher frequencies while PF samples behaved inversely (Table 7). The  $G'-G''$  crossover point corresponds to the characteristic elastic time of the composites describes as (44).

$$\lambda = \frac{G'}{G''\omega} \quad (1)$$

Where  $\omega$  is the oscillatory frequency (rad/s).

Figure 10 shows the normalized characteristic elastic time versus the filler content for both types of composites. The characterization elastic time of PF samples went up clearly as  $\text{CaF}_2$  content increased. While the characteristic elastic time of PC composites tended to decrease slightly by the increase of filler loading. This behavior can be related to better interaction of

CaF<sub>2</sub> particle with the polymer matrix which constrains movement ability of polymer chains and prolongs the relaxation times.

#### **4. Conclusion**

Calcium carbonate (CaCO<sub>3</sub>) is widely used in the polymer industry to reduce costs either via decreasing the processing energy and/or the cost of bulk materials. In this study, reclaimed calcium fluoride (CaF<sub>2</sub>), diverted from landfill, was introduced as a potential replacement for calcium carbonate. In this regard, PE/CaCO<sub>3</sub> (PC) and PE/CaF<sub>2</sub> (PF) composites were prepared in the wide range of filler content, i.e. 0-60 wt.%, through a parallel twin screw extruder. Standard samples then were made through injection process and their thermal, mechanical and rheological properties were studied in detail. Statistical analysis of thermal properties revealed that the enthalpy and crystallinity of the samples were independent from filler type and determined by filler content. Whereas, the most influential factors on yield stress of samples were the strain speed of the test and the filler type and the effect of filler content on the yield stress was not statistically significant. Overall, CaF<sub>2</sub> was more efficient in improving the mechanical properties of PE especially its young modulus compared to CaCO<sub>3</sub>. This could be thanks to the better interfacial interaction of CaF<sub>2</sub> with PE matrix which was observed through SEM images. Moreover, the dynamic mechanical analysis demonstrated that PF composites had higher dynamic mechanical properties at the ambient temperature compared to PC ones. The rheological investigation proved that the incorporation of calcium fluoride into PE for the amount of less than 40 wt% could decrease the complex viscosity of the melt and improve its flowability. Therefore it seems that due to its low price and functional performance, CaF<sub>2</sub> can be a promising alternative to CaCO<sub>3</sub> for the injection molding of PE parts.

#### **Acknowledgements**

This project has received funding from the European Union's Horizon 2020 research and innovation programme under the Marie Skłodowska-Curie grant agreement No. 847402.

**Declaration of conflicting interests**

The Author declare that there is no conflict of interest.

## References

1. Geyer R, Jambeck JR, Law KL. Production, use, and fate of all plastics ever made. *Sci Adv.* 2017 Jul;3(7):e1700782.
2. Maitz MF. Applications of synthetic polymers in clinical medicine. *Biosurface and Biotribology.* 2015 Sep;1(3):161–76.
3. Omar MF, Akil HM, Ahmad ZA. Effect of molecular structures on dynamic compression properties of polyethylene. *Mater Sci Eng A.* 2012 Mar;538:125–34.
4. Singh G, Klassen R, Howard J, Naudie D, Teeter M, Lanting B. Manufacturing, oxidation, mechanical properties and clinical performance of highly cross-linked polyethylene in total hip arthroplasty. *HIP Int.* 2018 Nov;28(6):573–83.
5. Espí E, Salmerón A, Fontecha A, García Y, Real AI. PLastic Films for Agricultural Applications. *J Plast Film Sheeting.* 2006 Apr;22(2):85–102.
6. Kasiri A, Rezaei M, Zandi F. The effect of polyethylene graft maleic anhydride compatibilizer on the physical, mechanical, and thermal properties of extruded noncross-linked low-density polyethylene nanocomposite foams. *J Thermoplast Compos Mater.* 2015;28(11):1537–49.
7. Horodytska O, Valdés FJ, Fullana A. Plastic flexible films waste management – A state of art review. *Waste Manag.* 2018 Jul;77:413–25.
8. Grand View Research. Injection Molded Plastics Market Size, Share & Trends Analysis Report By Raw Material (Polypropylene, ABS, HDPE, Polystyrene), By Application (Packaging, Electronics, Medical), And Segment Forecasts, 2019 - 2025.

- 2019.
9. Heidarbeigi J, Afshari H, Borghei AM. Study of physical and mechanical properties of PE/CNC nanocomposite for food packaging applications. *J Thermoplast Compos Mater.* 2021;34(3):396–408.
  10. Abeykoon C, Kelly AL, Vera-Sorroche J, Brown EC, Coates PD, Deng J, et al. Process efficiency in polymer extrusion: Correlation between the energy demand and melt thermal stability. *Appl Energy.* 2014 Dec;135:560–71.
  11. Burmann G, Fischer P, Michels R. ETA h High-Tech extrusion with barrier-mixing screws and spiral mandrel extrusion dies.
  12. Xanthos M. *Functional fillers for plastics.* Wiley-VCH; 2010. 507 p.
  13. Whiteman DJ, Agra-Gutierrez C, Bird MJ, Thomas SE, Skuse DR, Ansari DM. The Influence of Engineered Calcium Carbonate Functional Additives on the Mechanical Properties and Value Proposition of Polyethylene Films. *Polym Polym Compos.* 2011 Nov;19(9):743–52.
  14. Durand N, Monger HC, Canti MG, Verrecchia EP. Calcium Carbonate Features. In: *Interpretation of Micromorphological Features of Soils and Regoliths.* Elsevier; 2018. p. 205–58.
  15. Wu Z, Zhang Z, Mai K. Preparation and thermal property of ultrahigh molecular weight polyethylene composites filled by calcium carbonate modified with long chain. *J Thermoplast Compos Mater.* 2020;33(4):464–76.
  16. Gao F. *Advances in polymer nanocomposites: Types and applications.* Advances in



- Polymer Nanocomposites: Types and Applications. 2012. 1–651 p.
17. Magotra R, Namga S, Singh P, Arora N, Srivastava PK, Magotra R, et al. A New Classification Scheme of Fluorite Deposits. *Int J Geosci*. 2017 Apr;08(04):599–610.
  18. Lin MF, Wu JL, Chang KL, Lee WJ, Chang CP, Lin YC, Chen PH. Recycle of synthetic calcium fluoride and waste sulfuric acid to produce electronic grade hydrofluoric acid. *Environmental Science and Pollution Research*. 2020 Jul 29:1-7.
  19. Wang W, Blazek K, Cramb A. A Study of the Crystallization Behavior of a New Mold Flux Used in the Casting of Transformation-Induced-Plasticity Steels. *Metall Mater Trans B*. 2008 Feb;39(1):66–74.
  20. Feldmann C, Roming M, Trampert K. Polyol-Mediated Synthesis of Nanoscale CaF<sub>2</sub> and CaF<sub>2</sub>:Ce,Tb. *Small*. 2006 Nov;2(11):1248–50.
  21. Keaney E, Shearer J, Panwar A, Mead J. Refractive index matching for high light transmission composite systems. *J Compos Mater*. 2018 Oct;52(24):3299–307.
  22. Schrauwen BAG, Govaert LE, Meijer HEH. Toughness of high-density polyethylene with hard filler particles. 2000.
  23. Khalaf MN. Mechanical properties of filled high density polyethylene. *J Saudi Chem Soc*. 2015 Jan;19(1):88–91.
  24. Pedrazzoli D, Ceccato R, Karger-Kocsis J, Pegoretti A. Viscoelastic behaviour and fracture toughness of linear-low-density polyethylene reinforced with synthetic boehmite alumina nanoparticles. *Express Polym Lett*. 2013;7(8):652–66.
  25. Hall C. *Polymer Materials An Introduction for Technologists and Scientists*. Macmillan

- Education, Limited; 2017.
26. Aklonis JH, MacKnight WJ, Shen M, Mason WP. Introduction to Polymer Viscoelasticity. *Phys Today*. 2011;26(5):59–59.
  27. Razak JA, Akil HM, Ong H. Effect of inorganic fillers on the flammability behavior of polypropylene composites. *J Thermoplast Compos Mater*. 2007;20(2):195–205.
  28. Wohlford A, Walter T, Casem D, Moy P, Kidane A. Effects of Pressure and Strain Rate on the Mechanical Behavior of Glassy Polymers. In Springer, Cham; 2019. p. 259–62.
  29. Sutar H, Sahoo PC, Sahu PS, Sahoo S, Murmu R, Swain S, et al. Mechanical, Thermal and Crystallization Properties of Polypropylene (PP) Reinforced Composites with High Density Polyethylene (HDPE) as Matrix. *Mater Sci Appl*. 2018 May;09(05):502–15.
  30. Horvath T, Kalman M, Szabo T, Roman K, Zsoldos G, Szabone Kollar M. The mechanical properties of polyethylene-terephthalate (PET) and polylactic-acid (PDLLA and PLLA), the influence of material structure on forming. *IOP Conf Ser Mater Sci Eng*. 2018 Oct;426(1):012018.
  31. Kamal MR, Mutel A. Rheological Properties of Suspensions in Newtonian and Non-Newtonian Fluids. *J Polym Eng*. 1985 Jan;5(4):293–382.
  32. Yousfi M, Alix S, Lebeau M, Soulestin J, Lacrampe MF, Krawczak P. Evaluation of rheological properties of non-Newtonian fluids in micro rheology compounder: Experimental procedures for a reliable polymer melt viscosity measurement. *Polym Test*. 2014 Dec;40:207–17.
  33. Chung CI. *Extrusion of Polymers Theory & Practice* 2nd Edition.

34. Abraham TN, George KE. Short nylon fiber-reinforced HDPE: Melt rheology. *J Thermoplast Compos Mater.* 2009;22(3):293–304.
35. Crystan. Material Data Sheet, <https://www.crystran.co.uk/optical-materials/calcium-fluoride-caf2> (2012, accessed 02 June 2021)
36. Wang C, Chu M-C, Lin T-L, Lai S-M, Shih H-H, Yang J-C. Microstructures of a highly short-chain branched polyethylene. *Polymer (Guildf).* 2001 Feb;42(4):1733–41.
37. Hesabi M, Salimi A, Beheshty MH. Development of amine-based latent accelerator for one-pot epoxy system with low curing temperature and high shelf life. *Eur Polym J.* 2019 Mar;112:736–48.
38. Split-plot XI, Xi B. Design and analysis of experiments-. In 2006. p. 135–41.
39. S. Hobeika, Y. Men and, Strobl\* G. Temperature and Strain Rate Independence of Critical Strains in Polyethylene and Poly(ethylene-co-vinyl acetate). 2000;
40. Hiss R, Hobeika S, Lynn C, Strobl G. Network stretching, slip processes, and fragmentation of crystallites during uniaxial drawing of polyethylene and related copolymers. A comparative study. *Macromolecules.* 1999;32(13):4390–403.
41. Ahsan T, Taylor DA. The Influence of Surface Energetics of Calcium Carbonate Minerals on Mineral-Polymer Interaction in Polyolefin Composites. *J Adhes.* 1998;67(1–4):69–79.
42. Sanchez-Leija RJ, Riba-Moliner M, Cayuela-Marín D, Dominguez-Espinos O, Sanchez-Loredo MG. Surface Modification of a Calcium Fluoride Filler and the Effect on the Nonisothermal Crystallization Behavior of Poly(ethylene terephthalate). *Polym Eng Sci.*

2014;54(12):2938–46.

43. De Leeuw NH, Cooper TG. A computational study of the surface structure and reactivity of calcium fluoride. *J Mater Chem.* 2003;13(1):93–101.
44. Rueda MM, Fulchiron R, Martin G, Cassagnau P. Rheology of polypropylene filled with short-glass fibers: From low to concentrated filled composites. *Eur Polym J.* 2017 Aug;93:167–81.

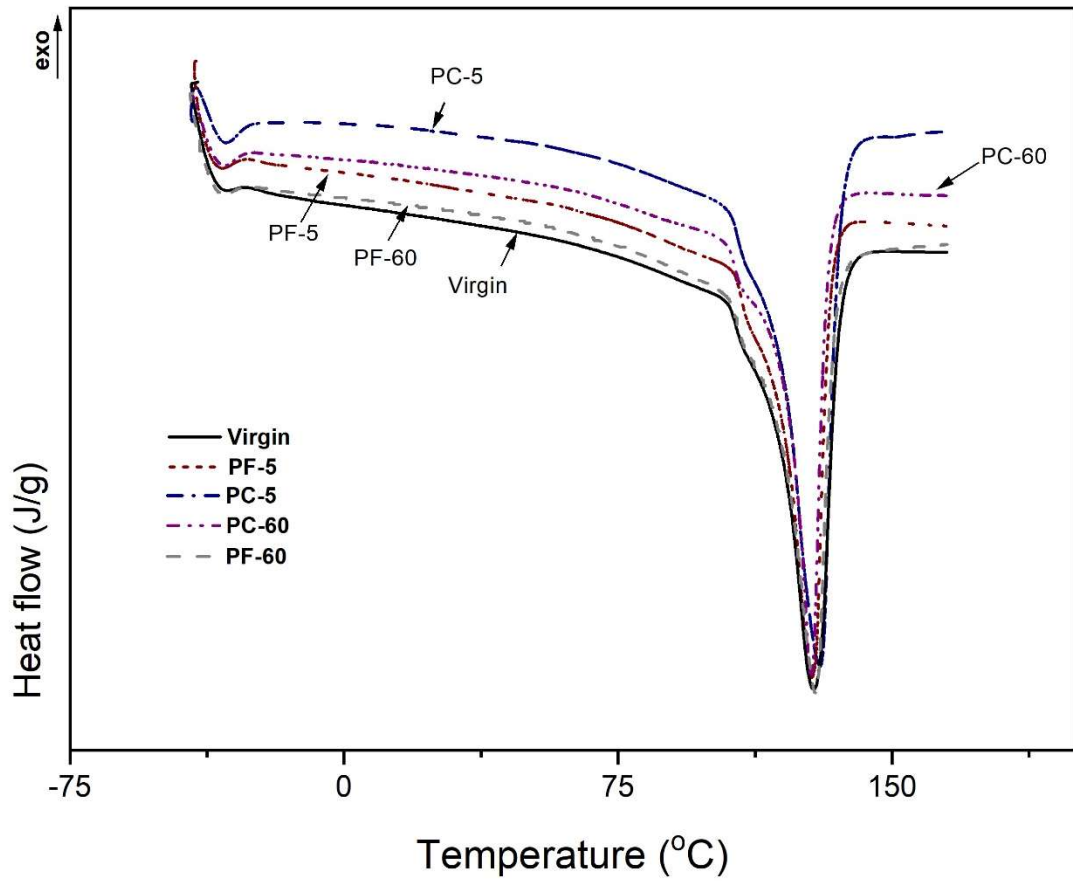


Figure 1- DSC thermograms of virgin PE and its composites with calcium carbonate and calcium fluoride at the heating of 10 °C/min

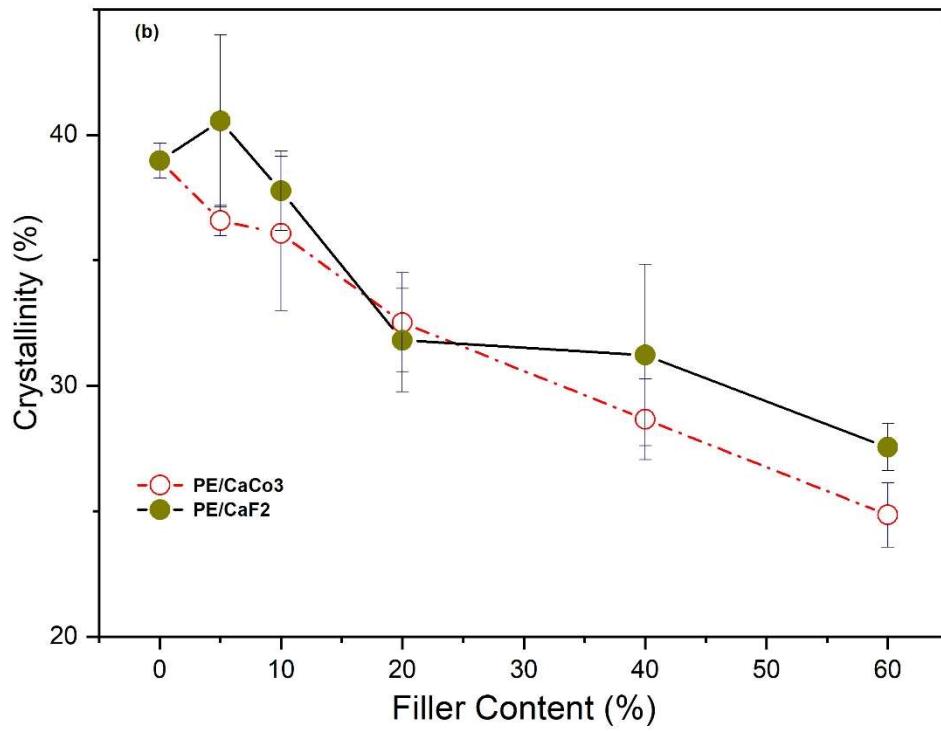
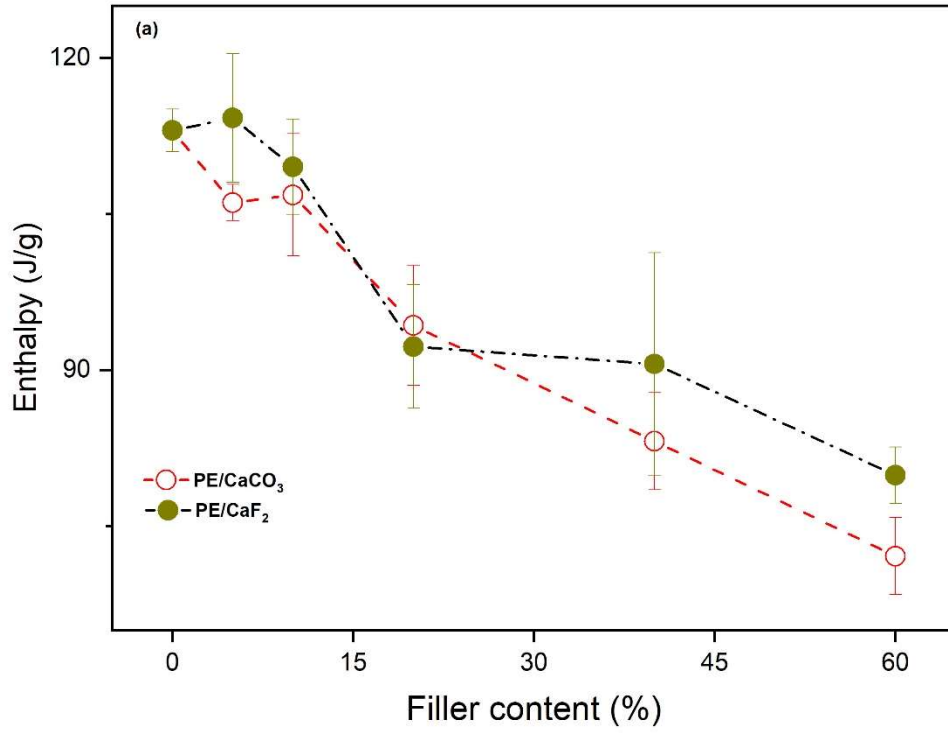


Figure 2- Comparison of the effect of inorganic fillers type and content on (a) the enthalpy level and (b) the crystallinity of PE composites

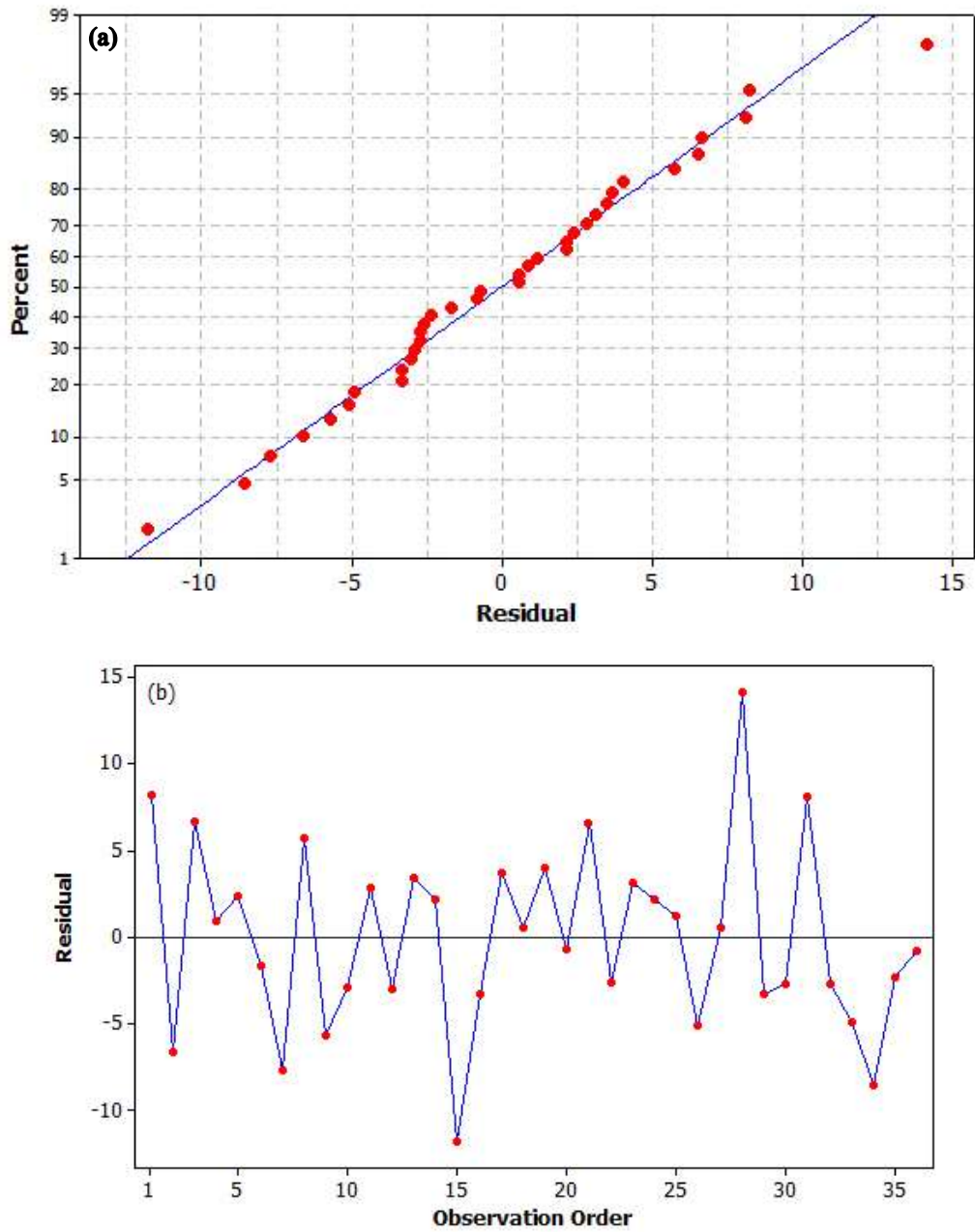


Figure 3- (a) Normal probability plot and (b) residuals vs. observation order of the response of enthalpy

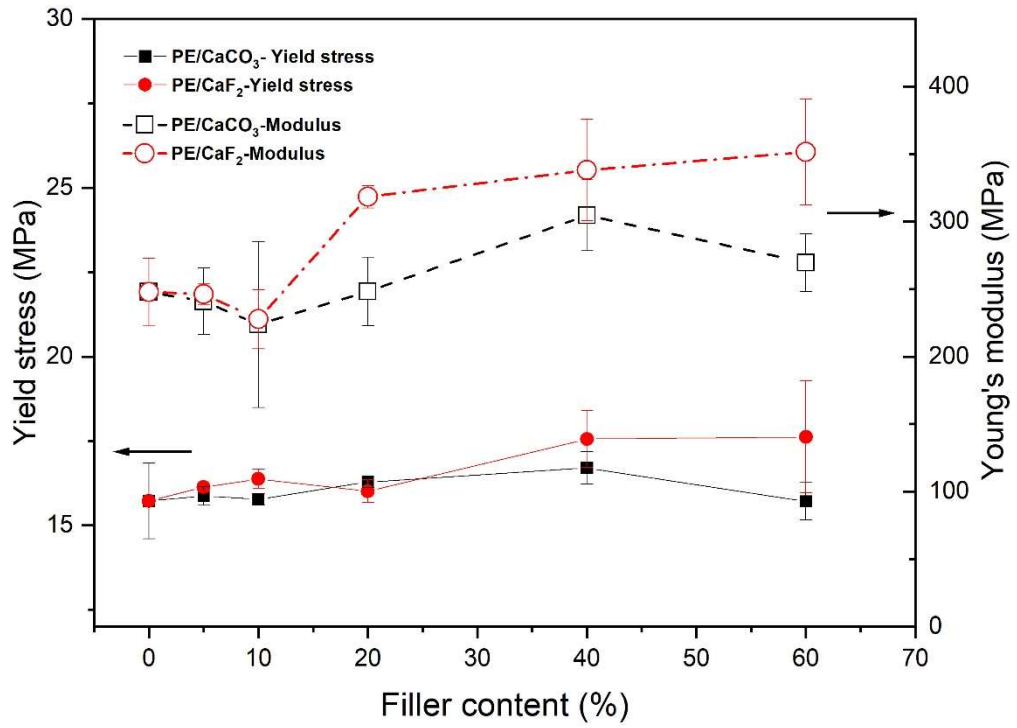


Figure 4- The variation of yield stress and Young modulus as a function of filler content for PE/CaCO<sub>3</sub> and PE/CaF<sub>2</sub> composites



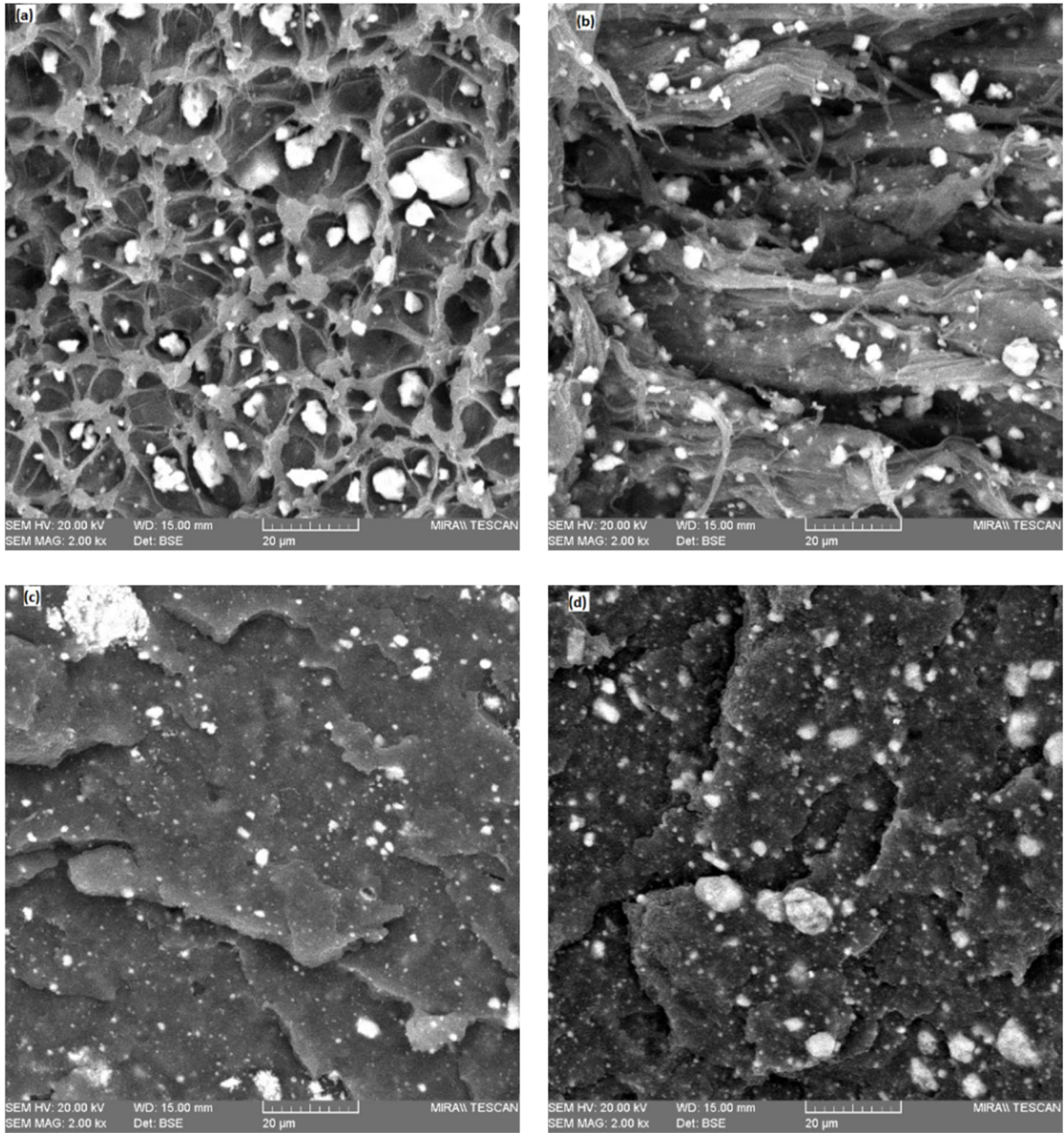


Figure 5- SEM micrographs of (a) PC 20 (b) PC 60 (c) PF20 and (d) PF 60. The photomicrographs were obtained with an identical magnification.

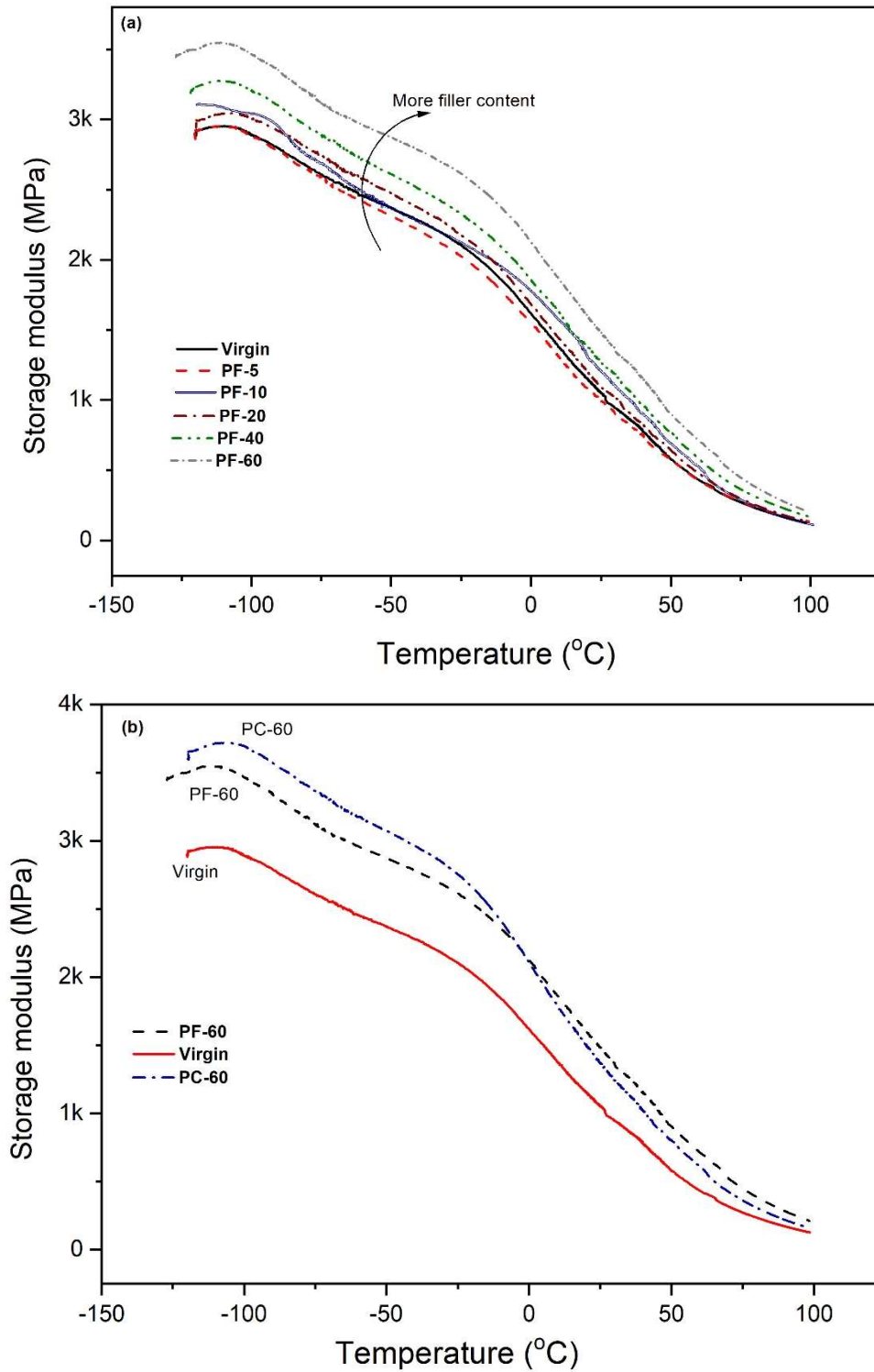


Figure 6- Temperature dependence of storage modulus of (a) PE/CaF<sub>2</sub> composites (b) PF-60, PC-60 and virgin PE

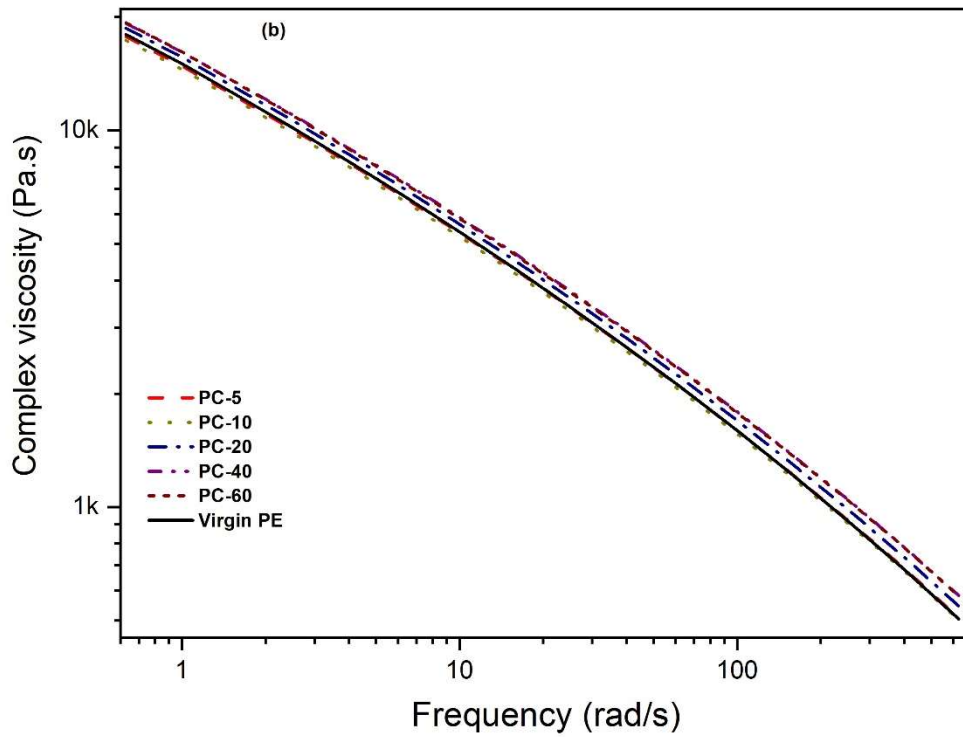
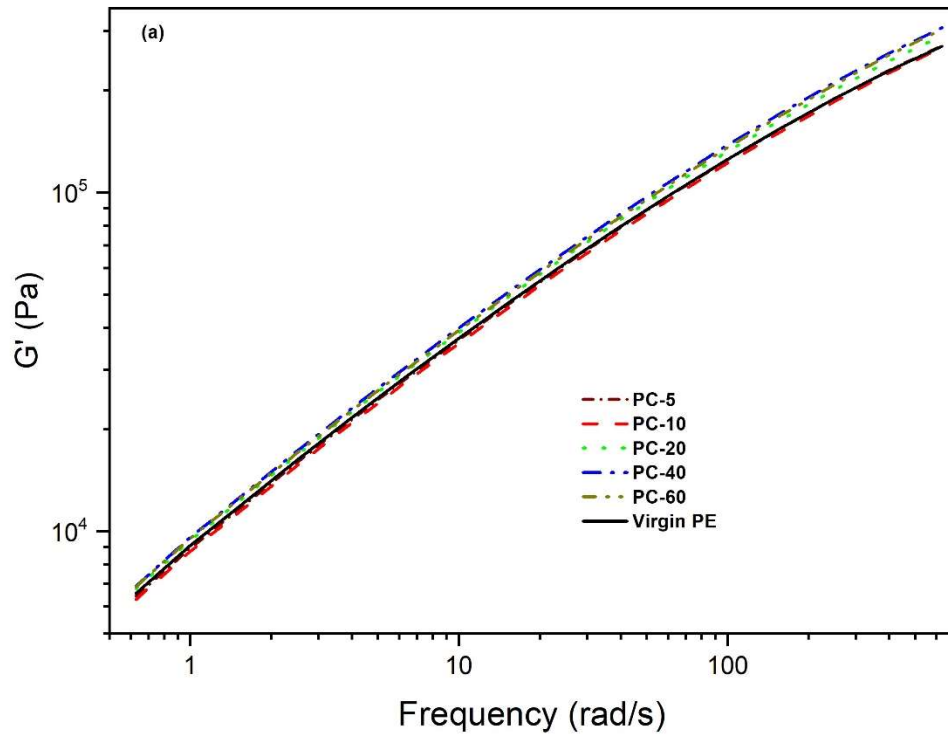


Figure 7- Dynamic rheological characteristics of PE/CaCO<sub>3</sub> (a) storage modulus (b) complex viscosity

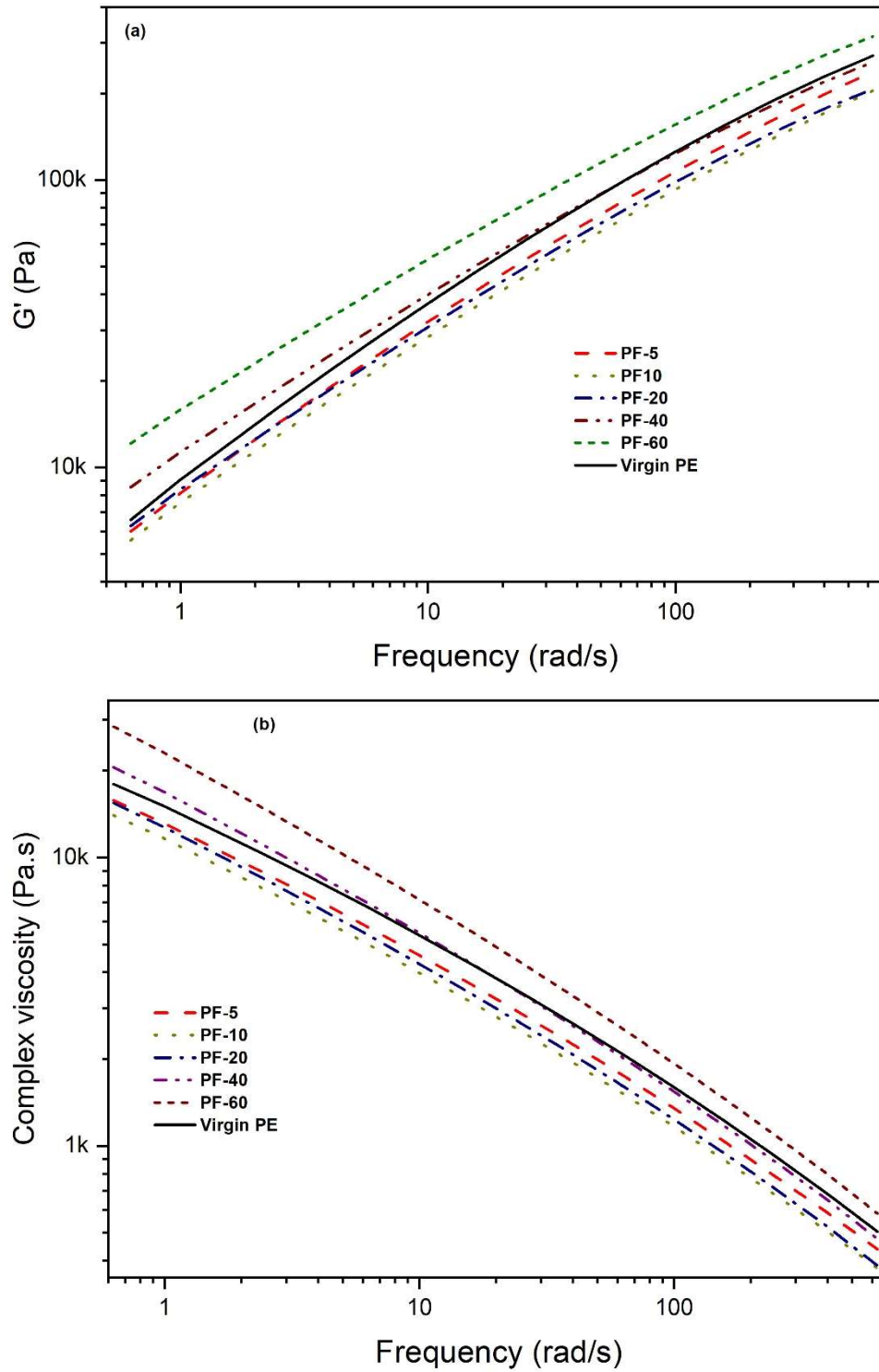


Figure 8- Dynamic rheological characteristics of PE/CaF<sub>2</sub> (a) storage modulus (b) complex viscosity

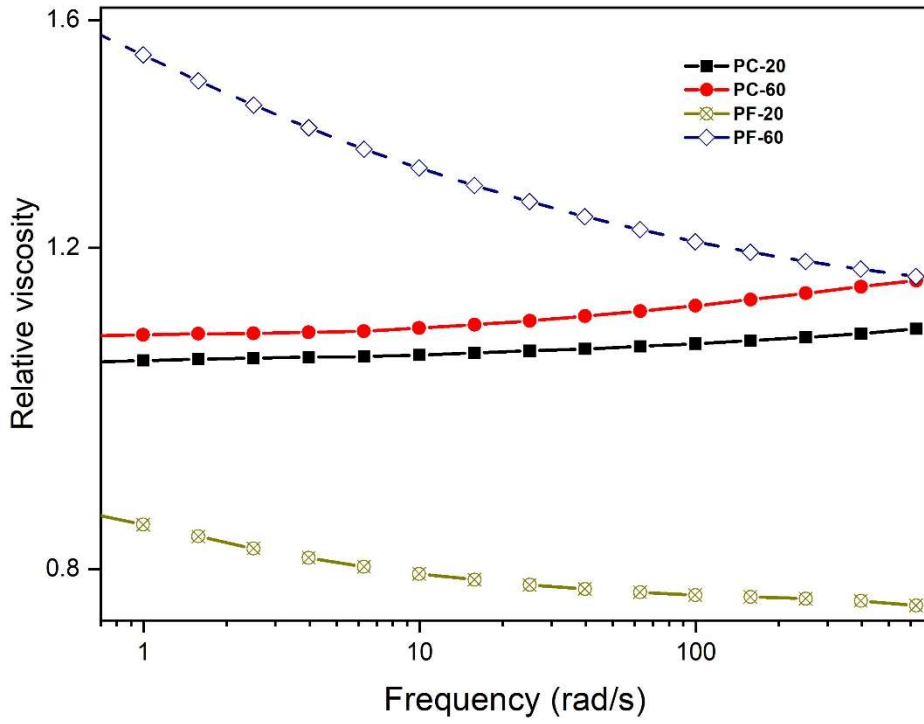


Figure 9- Relative viscosity composites as a function of frequency for PC and PF samples

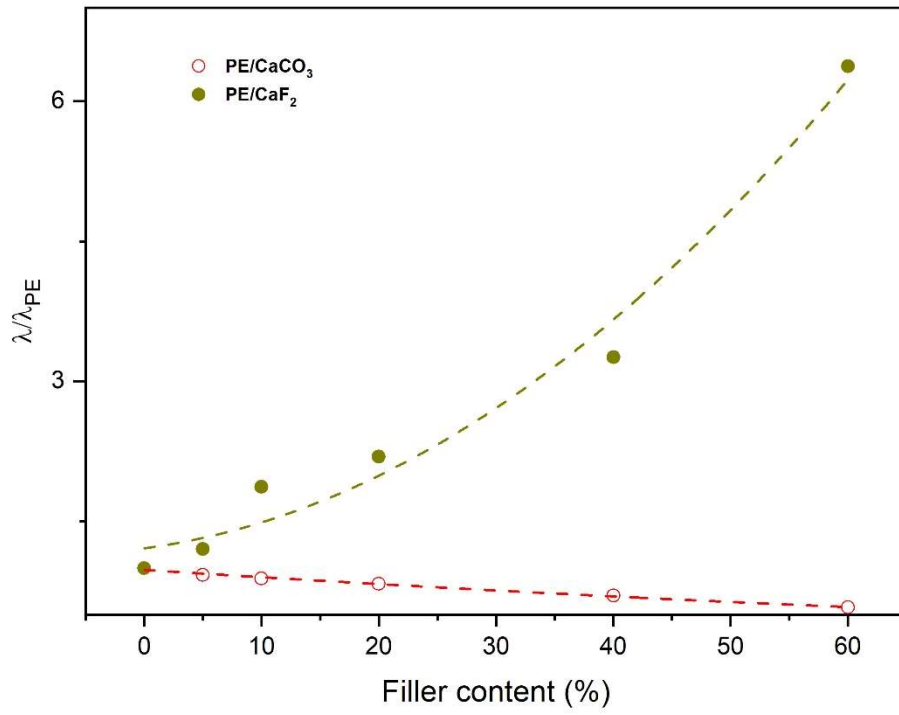


Figure 10- Normalized characteristic elastic time as a function of the filler content

Table 1- The corresponding notations of composites

| <b>Filler weight percentage</b> | <b>5</b> | <b>10</b> | <b>20</b> | <b>40</b> | <b>60</b> |
|---------------------------------|----------|-----------|-----------|-----------|-----------|
| PE/calcium carbonate (PC)       | PC-5     | PC-10     | PC-20     | PC-40     | PC60      |
| PE/calcium fluoride (PF)        | PF-5     | PF-10     | PF-20     | PF-40     | PF-60     |

Table 2- DSC data for PE/CaCO<sub>3</sub> and PE/CaF<sub>2</sub> composites at the heating rate of 10 °C/min

|                      | <b>Virgin</b> | <b>PC-5</b> | <b>PC-10</b> | <b>PC-20</b> | <b>PC-40</b> | <b>PC-60</b> | <b>PF-5</b> | <b>PF-10</b> | <b>PF-20</b> | <b>PF-40</b> | <b>PF-60</b> |
|----------------------|---------------|-------------|--------------|--------------|--------------|--------------|-------------|--------------|--------------|--------------|--------------|
| <b>T<sub>m</sub></b> | 116.7         | 120.0       | 119.1        | 117.0        | 117.5        | 119.4        | 117.1       | 117.2        | 117.8        | 117.7        | 116.8        |
| <b>(onset)</b>       | ± 0.4         | ± 0.2       | ± 2.7        | ± 0.2        | ± 0.7        | ± 1.8        | ± 0.3       | ± 0.0        | ± 0.3        | ± 0.6        | ± 0.4        |
| <b>T<sub>m</sub></b> | 128.5         | 130.4       | 129.3        | 130.0        | 127.8        | 128.6        | 129.1       | 128.9        | 128.8        | 128.5        | 128.5        |
| <b>(peak)</b>        | ± 0.9         | ± 0.0       | ± 0.5        | ± 0.7        | ± 0.4        | ± 0.6        | ± 0.8       | ± 0.0        | ± 0.5        | ± 0.1        | ± 0.9        |



Table 3- Analysis of variance for Enthalpy

| Source              | DF | Sum of squares | Mean squares | F            | P-value | Contribution (%) |
|---------------------|----|----------------|--------------|--------------|---------|------------------|
| Filler type (FT)    | 1  | 141.81         | 141.81       | 3.41         | 0.077   | 0.02             |
| Filler content (FC) | 5  | 6643.20        | 1328.64      | <b>31.93</b> | 0.000   | 0.84             |
| FT*FC interaction   | 5  | 147.13         | 29.43        | 0.71         | 0.624   | 0.02             |
| Error               | 24 | 998.75         | 41.61        | -            | -       | 0.13             |
| Total               | 35 | 7930.89        |              | -            | -       | 100              |

DF: Degree of Freedom

Table 4- Analysis of variance for crystallinity

| Source              | DF | Sum of squares | Mean squares | F            | P-value | Contribution (%) |
|---------------------|----|----------------|--------------|--------------|---------|------------------|
| Filler type (FT)    | 1  | 26.09          | 26.09        | 4.03         | 0.056   | 0.03             |
| Filler content (FC) | 5  | 806.02         | 161.20       | <b>24.87</b> | 0.000   | 0.80             |
| FT*FC interaction   | 5  | 23.27          | 4.65         | 0.72         | 0.616   | 0.02             |
| Error               | 24 | 155.56         | 6.48         | -            | -       | 0.15             |
| Total               | 35 | 1010.90        | -            | -            | -       | 100              |

Table 5- Analysis of Variance for yield stress response

| Source              | DF       | Sum of squares | Mean squares | F             | P-value     | Contribution (%) |      |
|---------------------|----------|----------------|--------------|---------------|-------------|------------------|------|
| Filler type (FT)    | 1        | 17.366         | 17.366       | <b>32.92</b>  | 0.000       | 0.05             |      |
| Filler content (FC) | 5        | 13.311         | 2.662        | 5.05          | 0.000       | 0.04             |      |
| Strain speed (SS)   | 1        | 242.078        | 242.078      | <b>458.84</b> | 0.000       | 0.71             |      |
| Interactions        | FT*FC    | 5              | 11.449       | 2.290         | <b>4.34</b> | 0.001            | 0.03 |
|                     | FT*SS    | 1              | 1.867        | 1.867         | 3.54        | 0.063            | 0.01 |
|                     | FC*SS    | 5              | 1.860        | 0.372         | 0.71        | 0.621            | 0.01 |
|                     | FT*FC*SS | 5              | 0.555        | 0.111         | 0.21        | 0.957            | 0.00 |
| Error               | 96       | 50.648         | 0.528        | -             | -           | 0.15             |      |
| Total               | 119      | 339.134        | -            | -             | -           | 100              |      |

Table 6- Analysis of variance for Young's modulus

| Source              | DF       | Sum of squares | Mean squares | F            | P-value     | Contribution (%) |      |
|---------------------|----------|----------------|--------------|--------------|-------------|------------------|------|
| Filler type (FT)    | 1        | 28244          | 28244        | <b>27.58</b> | 0.000       | 0.06             |      |
| Filler content (FC) | 5        | 185068         | 37014        | <b>36.14</b> | 0.000       | 0.38             |      |
| Strain speed (SS)   | 1        | 82713          | 82713        | <b>80.77</b> | 0.000       | 0.17             |      |
| Interactions        | FT*FC    | 5              | 36430        | 7286         | <b>7.11</b> | 0.000            | 0.08 |
|                     | FT*SS    | 1              | 3630         | 3630         | 3.54        | 0.063            | 0.01 |
|                     | FC*SS    | 5              | 33711        | 6742         | <b>6.58</b> | 0.000            | 0.07 |
|                     | FT*FC*SS | 5              | 16375        | 3275         | <b>3.2</b>  | 0.010            | 0.03 |
| Error               | 96       | 98308          | 1024         | -            | -           | 0.20             |      |
| Total               | 119      | 484479         | -            | -            | -           | 100              |      |

Table 7- Dynamic Mechanical Properties of PE/CaCO<sub>3</sub> and PE/CaF<sub>2</sub> composites at ambient temperature

| <b>Samples</b>           | <b>Virgin</b> | <b>PC-5</b> | <b>PC-10</b> | <b>PC-20</b> | <b>PC-40</b> | <b>PC-60</b> | <b>PF-5</b> | <b>PF-10</b> | <b>PF-20</b> | <b>PF-40</b> | <b>PF-60</b> |
|--------------------------|---------------|-------------|--------------|--------------|--------------|--------------|-------------|--------------|--------------|--------------|--------------|
| <b>DMA Properties</b>    |               |             |              |              |              |              |             |              |              |              |              |
| Stiffness (N/m, @ 30 °C) | 14284         | 15180       | 15705        | 14709        | 16927        | 18895        | 13688       | 14274        | 15423        | 17835        | 20656        |
| G' (MPa, @ 30 °C)        | 942           | 1039        | 1152         | 1005         | 1117         | 1246         | 903         | 942          | 1017         | 1176         | 1363         |
| G'' (MPa, @30 °C)        | 101           | 115         | 131          | 112          | 122          | 134          | 95          | 98           | 106          | 119          | 135          |
| Crossover Point (rad/s)  | 14.4          | 15.6        | 16.2         | 17.4         | 20.4         | 25.0         | 11.9        | 7.7          | 6.6          | 4.4          | 2.3          |